JOURNAL OF MATERIALS SCIENCE **34** (1999) 2971–2978

Effect of iron content and annealing temperature on the corrosion behavior of $Ni_{100-x}Fe_x$

E. F. EL-WAHIDY, A. I. ABOU-ALY, N. G. GOMAA, S. F. ABAZA
Department of Physics, Faculty of Science, Alexandria University, Alex., Egypt

$Ni_{100-x}Fe_x$ metallic glasses have been prepared with $8.5 \leq x \leq 51$ using electrodeposition technique. Corrosion behavior of specimens in 0.1 M Na_2SO_4 (pH = 6) at 25 °C has been studied using potential-time decay, linear polarization resistance and potentiodynamic techniques. Anodic polarization curves show that the specimens exhibit quasi-passive region. The dissolution of samples increases with the increase of iron concentration and also with the increase of annealing temperature. The interpretation was based on the enhanced dissolution of the formed microcrystals of the specimens in the sulphate solution.

1. Introduction

Nickel-iron alloy may be formed by different techniques such as sputtering [1], vapor deposition [2] and electrodeposition [3]. The electrodeposition of Ni-Fe alloy deposits from both sulphate and chloride baths and their mechanical properties are discussed in detail as a function of both composition and current density [4]. Ni-Fe alloy exhibits anomalous codeposition [5], i.e., the less noble metal, Fe, deposits preferentially to the more noble metal, Ni.

The study of Ni-Fe alloy gains its importance in recent years because it has a number of applications as magnetic [6], decorative [7], and electroformed material [8]. Such applications require uniform and constant physico-chemical properties of the alloy deposits. However, in general, the composition of Ni-Fe alloys is affected dramatically by current density, agitation and other plating variables [9].

Homogeneous amorphous alloys that lack grain boundaries, dislocation or inclusions are less prone to corrosive attack because the corrosion process seems to occur more often at such sites in crystalline materials [10]. Studies by Reverz and Kruger [11] indicate that amorphous films have greater corrosion resistance than their crystalline counterparts.

This work investigates the effect of increase of iron content and annealing temperature on the behavior of corrosion of $Ni_{100-x}Fe_x$ at $8.5 \leq x \leq 51$.

2. Experimental

2.1. Samples preparation

Samples of $Ni_{100-x}Fe_x$ were prepared by electrodeposition. Bath compositions reported by Nakamura and Hayashi [12] are given in Table I. A d.c. power supply was used to maintain a plating current density of 300 mA/cm^2, the temperature of the solution was maintained constant at 50 °C and the plating time was 3 hours.

The cathode was copper sheet (0.27 mm thick), embedded in epoxy material which does not react with the chemicals used in the electrodeposition process, leaving an exposed window [0.7 cm^2] to react with the corrosive medium. The substrate was first mechanically polished with a series of emery papers starting with a coarse one and proceeding in steps to finer grades, then the substrate were chemically polished using a solution of 55% phosphoric acid, 25% acetic acid and 20% nitric acid. After completion of the plating, the sample was easily to be stripped directly from the cathode without any chemical treatment which been used in other system. The resulting samples were generally flat, smooth and bright. Annealing of samples was carried out in furnace at 500 and 700 °C at atmospheric pressure. Then sample was furnace-cooled to the room temperature. Iron percentage in the samples was determined by Atomic Absorption Spectrophotometer (Perkin Elmer 2380). The results are listed in Table II.

2.2. Corrosion testing

The corrosion potential of the working electrode was recorded as a function of time with respect to saturated calomel electrode (SCE) using AMEL differential electrometer model 621. Platinum wire served as an auxiliary electrode. Polarization resistance and potentiodynamic scanning methods were used to characterize corrosion performance. The potentiodynamic polarization of samples were measured at the applied volt was increasing with steps 20 mV and then the stability was achieved with 60 s by using AMEL potentiostate model 55. Immersion time before performing the measurements was 50 min, and the measuring temperature was kept constant at 25 °C.

3. Results and discussion

The corrosion of $Ni_{100-x}Fe_x$ alloys in 0.1 M Na_2SO_4 (pH = 6) aqueous solution was studied by using

TABLE I Bath compositions and deposition parameters for the electrodeposition

Bath composition	
$NiSO_4{\cdot}6H_2O$	85 g/l
$NiCl_2{\cdot}6H_2O$	135 g/l
H_3BO_3	50 g/l
Saccharin	0.4 g/l
Citric Acid	0.06 g/l
$FeSO_4{\cdot}7H_2O$	10 : 80 g/l
Deposition parameters	
Temperature	50 °C
Current density	300 mA/cm^2
Plating time	3 h

TABLE II Concentration of Fe in the $Ni_{100-x}Fe_x$ alloys

Fe (at %)	$FeSO_4{\cdot}6H_2O$ (g/l)
8.5	10
18.5	20
25.5	40
45	60
51	80

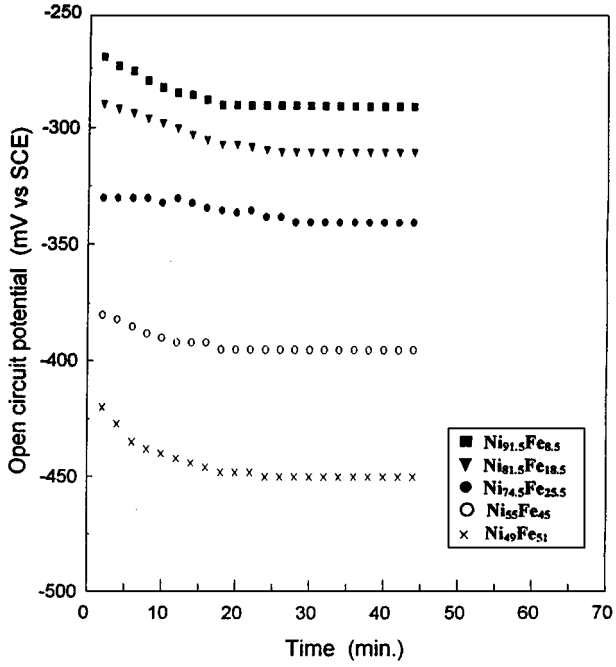

Figure 1 Open circuit potential vs. time for $Ni_{100-x}Fe_x$ at $8.5 \leq x \leq 51$ in 0.1 M Na_2SO_4 solution. (■) $Ni_{91.5}Fe_{8.5}$, (▼) $Ni_{81.5}Fe_{18.5}$, (●) $Ni_{74.5}Fe_{25.5}$, (○) $Ni_{55}Fe_{45}$ and (×) $Ni_{49.5}Fe_{51.5}$.

potential-time decay, potentiodynamic polarization and the linear polarization resistance techniques. The measurements were carried out for five concentrations of $Ni_{100-x}Fe_x$ and annealing temperatures at (T_{an}) 500 and 700 °C.

3.1. Effect of increasing iron content on the corrosion of $Ni_{100-x}Fe_x$ alloy

Potential-time curves obtained for electroplating $Ni_{100-x}Fe_x$ at $8.5 \leq x \leq 51$ are presented in Fig. 1. The

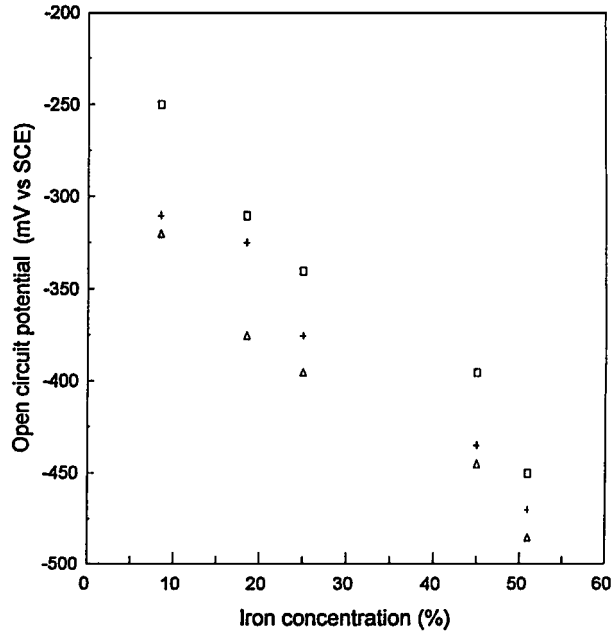

Figure 2 Open circuit potential vs. iron percentage with and without annealing temperature for Ni-Fe alloys immersed in 0.1 M Na_2SO_4 solution. (□) without annealing, (+) $T_{an} = 500$ °C and (Δ) $T_{an} = 700$ °C.

examined specimens showed no significant displacement of the open circuit potential ($E_{o.c}$) for a period of forty five minutes upon immersion in the sulphate. The $E_{o.c}$ decreases as the concentration of iron increases. Fig. 2 represents the change of the $E_{o.c}$ as a function of the iron concentration in the alloys at different annealing temperatures. Samples without annealing showed a decrease of $E_{o.c}$ with increasing the iron content is observed, i.e., corrosion resistance of the samples decrease at high iron concentration.

To investigate the mechanism of the corrosion of the specimens, the potentiodynamic polarization curves for $Ni_{100-x}Fe_x$ alloys are measured and represented in Fig. 3. This technique is achieved by measuring the potential-current curves (Tafel plots) in both anodic and cathodic direction. It was pointed out that during the application of potentiodynamic technique to evaluate corrosion rate, attention should be paid to choose "correct" scan rate for determining the polarization characteristics [13]. Mansfeld and Kending [14] have found that, the reasonable data can be obtained for scan rate less than 1 mV/s.

Fig. 3 shows that the potentiodynamic polarization curves for different samples are nearly identical through cathodic polarization, while the difference has been observed in the anodic polarization behavior of samples. The potential region, at which the current is approximately stable "quasi-passive", exists in some of the examined specimens. It is known that crystalline nickel exhibits a passive region [15] in its polarization characteristics. On the other hand the iron does not exhibit such region, therefore the Ni-Fe system is considered as a complex system. Consequently, the existence of the quasi passive region for the different samples are irregular. Also the existence of quasi-passive region may be related to the existence of microcrystallites of Ni_3Fe within the amorphous matrix.

TABLE III Electrochemical parameters obtained from d.c. measurements of electrodeposited $Ni_{100-x}Fe_x$ in 0.1 M Na_2SO_4

Fe%	T_{an}(°C)	$E_{o.c}$(mV)	i_{corr}(μA/cm^2)	$(i_{corr})_A/(i_{corr})_B$	R_p ($10^3 \times \Omega$)	$(1/R_p)_A/(1/R_p)_B$
8.5	Without	−290	1.34	—	111.0	—
	500	−310	3.05	2.27	52.38	2.11
	700	−320	4.25	3.17	34.67	3.20
18.5	Without	−310	1.70	—	82.00	—
	500	−325	3.05	1.79	42.34	1.93
	700	−375	5.08	2.98	27.65	2.96
25.5	Without	−340	3.50	—	42.30	—
	500	−375	5.60	1.60	28.56	1.48
	700	−395	8.22	2.34	20.15	2.09
45	Without	−395	7.70	—	27.37	—
	500	−435	10.90	1.41	20.77	1.31
	700	−445	12.96	1.68	17.30	1.58
51	Without	−450	9.06	—	20.07	—
	500	−470	11.60	1.28	16.07	1.24
	700	−480	14.20	1.56	13.31	1.50

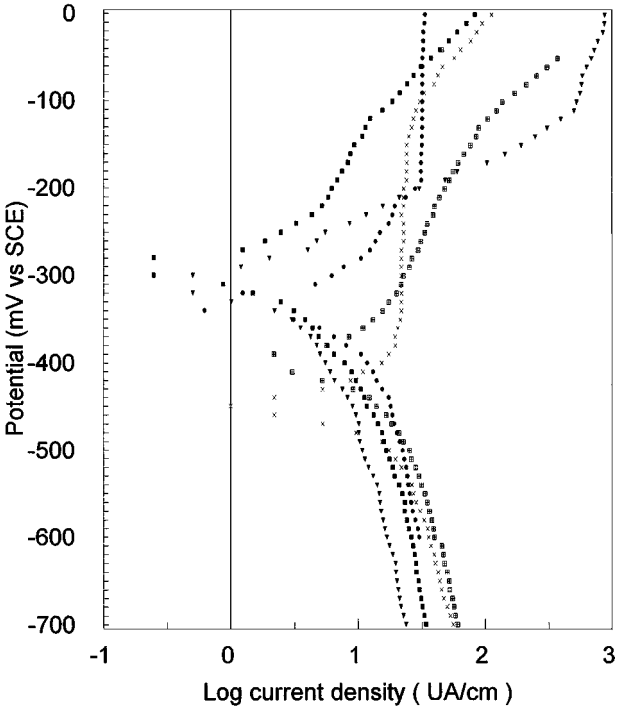

Figure 3 Potentiodynamic polarization curves for $Ni_{100-x}Fe_x$ at $8.5 \leq x \leq 51$ in 0.1 M Na_2SO_4 solution. (■) $Ni_{91.5}Fe_{8.5}$, (▼) $Ni_{81.5}Fe_{18.5}$, (●) $Ni_{74.5}Fe_{25.5}$, (⊞) $Ni_{55}Fe_{45}$ and (×) $Ni_{49.5}Fe_{51.5}$.

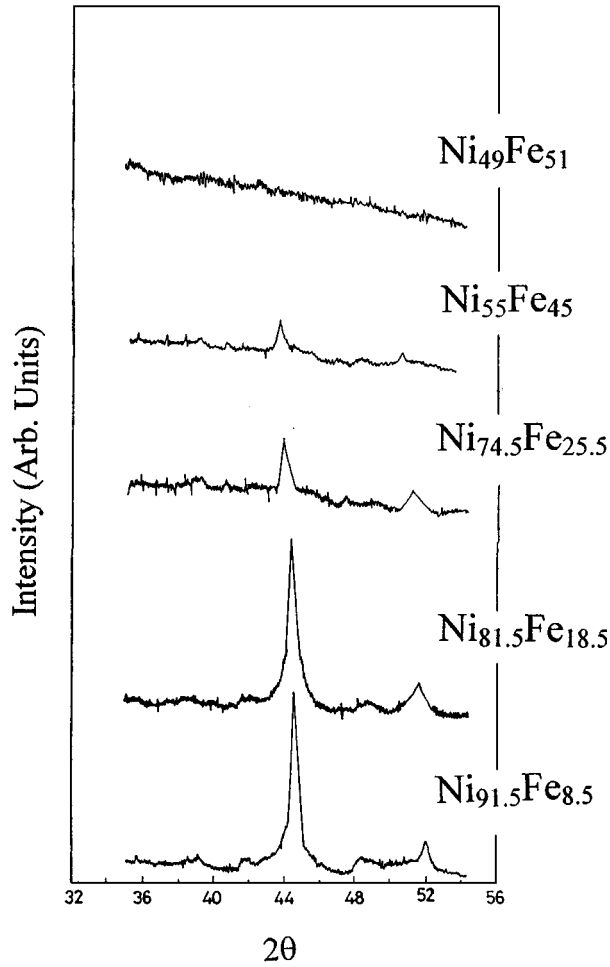

Figure 4 X-ray scans of $Ni_{100-x}Fe_x$ alloy at $8.5 \leq x \leq 18.5$ without annealing.

Meaningful parameters obtained from the potentiodynamic polarization curves for different iron percentage are presented in Table III. This includes the open circuit potential ($E_{o.c}$), the corrosion current density (I_{corr}) and the polarization resistance (R_p). The experimental data in Table III show that, in the active region, the corrosion current generally increases in samples with high iron concentrations. The X-Ray diffractograms of these samples indicate that the amorphous state increases with the increase in iron concentration [16] (X-ray diffractions are presented in Fig. 4 just to show the change in crystallinity).

In order to explain above results, it was assumed that there are two factors which affect the corrosion mechanism of Ni-Fe alloy. The first factor tends to increase the corrosion rate of Ni-Fe due to the increase existence of Fe content. While the second one tends to decrease the corrosion rate. This decrease is attributed to the increase in the amorphous phase of the sample. Since the increase of the iron content in the sample leads to a marked sever reduction in its crystalline state, as indicated by the X-ray diffractogram [16], then there is a lack of grain boundaries and hence the corrosion rate decreases. From Table III, it can be noticed that the corrosion current of the samples slightly increases as

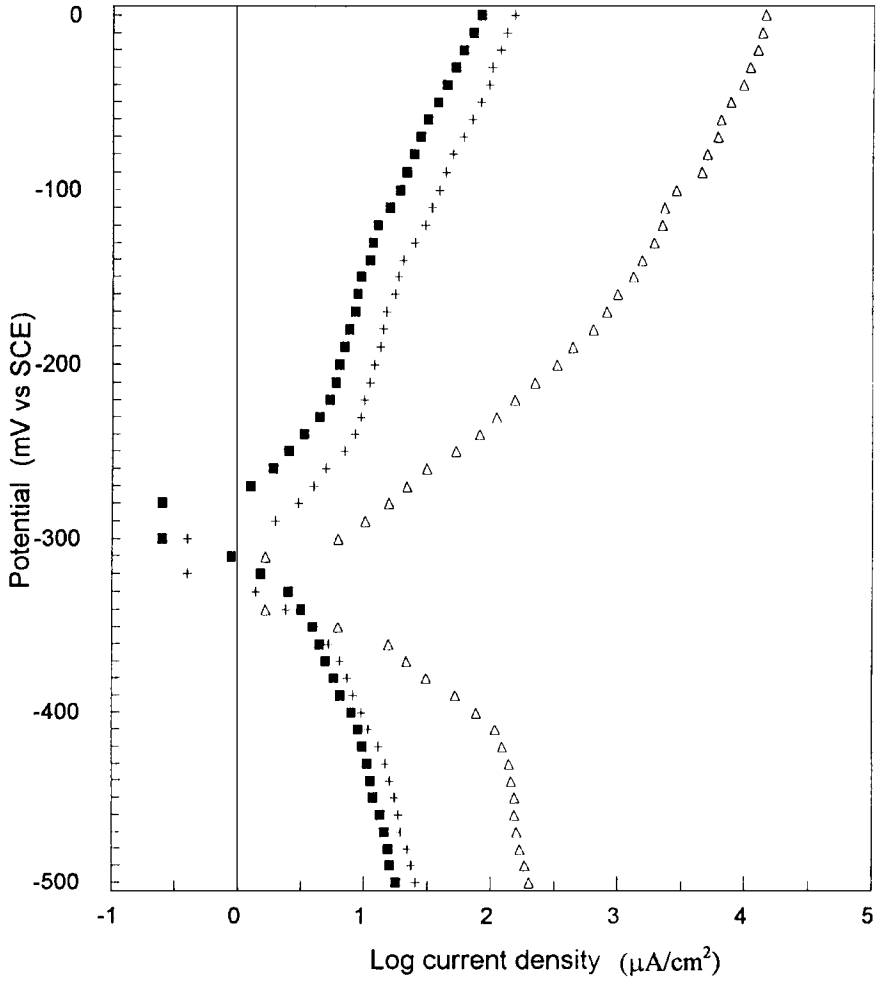

Figure 5 Potentiodynamic polarization curves for $Ni_{91.5}Fe_{8.5}$ in 0.1 M Na_2SO_4 solution at different annealing temperature. (■) without annealing, (+) $T_{an} = 500\,^{\circ}C$ and (△) $T_{an} = 700\,^{\circ}C$.

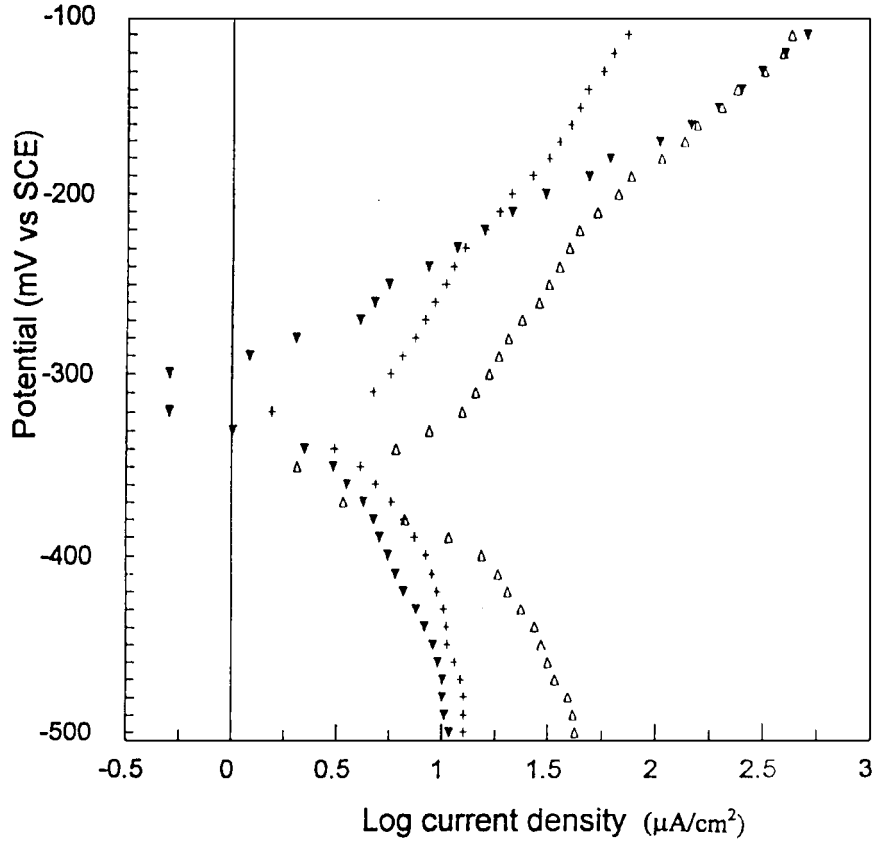

Figure 6 Potentiodynamic polarization curves for $Ni_{81.5}Fe_{18.5}$ in 0.1 M Na_2SO_4 solution at different annealing temperature. (▼) without annealing, (+) $T_{an} = 500\,^{\circ}C$ and (△) $T_{an} = 700\,^{\circ}C$.

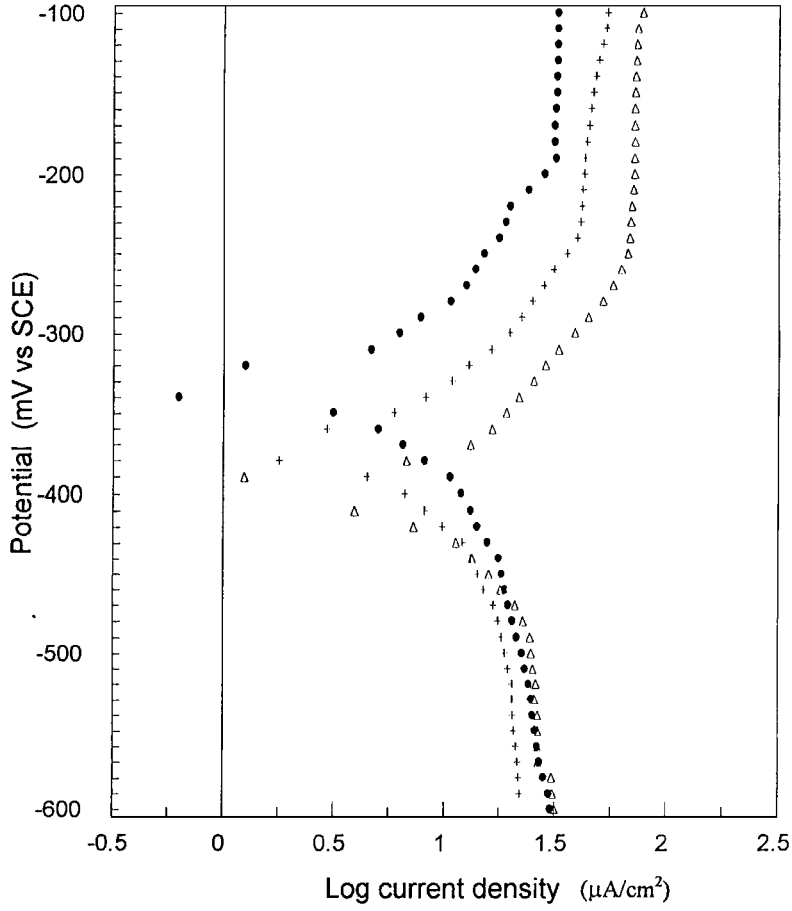

Figure 7 Potentiodynamic polarization curves for $Ni_{74.5}Fe_{25.5}$ in 0.1 M Na_2SO_4 solution at different annealing temperature. (●) without annealing, (+) $T_{an} = 500\,^{\circ}C$ and (△) $T_{an} = 700\,^{\circ}C$.

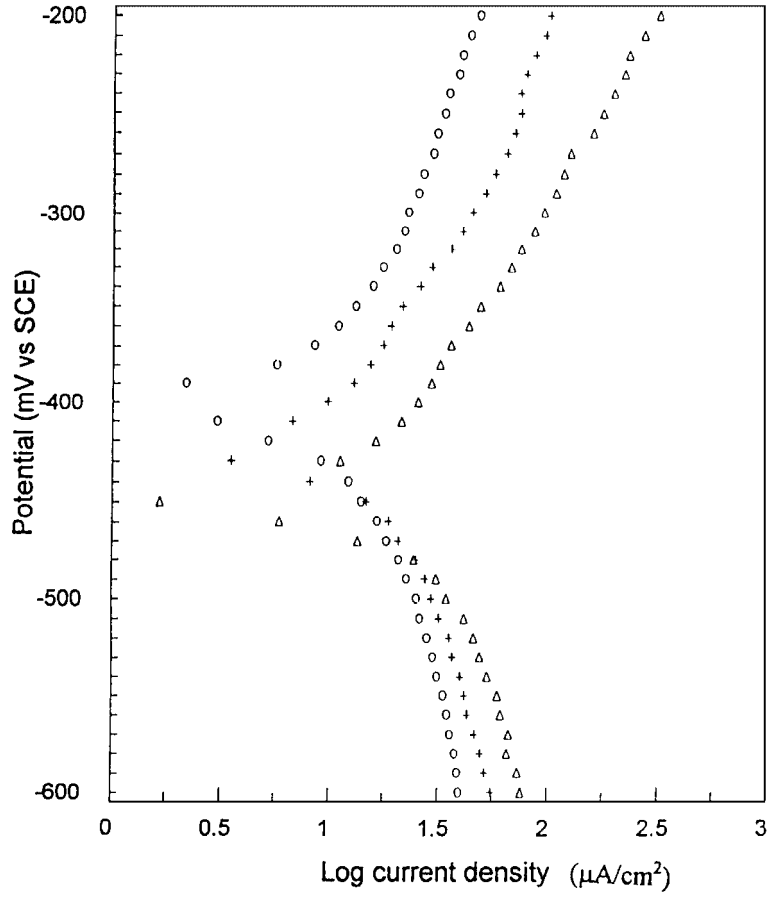

Figure 8 Potentiodynamic polarization curves for $Ni_{55}Fe_{45}$ in 0.1 M Na_2SO_4 solution at different annealing temperature. (□) without annealing, (+) $T_{an} = 500\,^{\circ}C$ and (△) $T_{an} = 700\,^{\circ}C$.

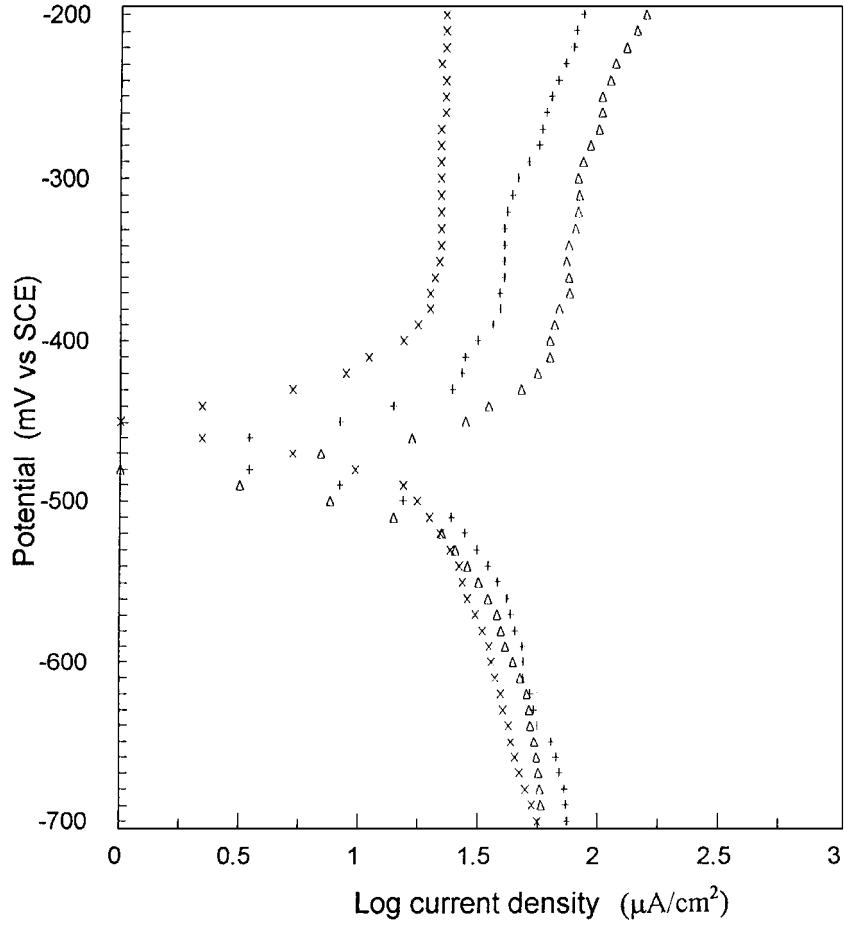

Figure 9 Potentiodynamic polarization curves for $Ni_{49}Fe_{51}$ in 0.1 M Na_2SO_4 solution at different annealing temperature. (×) without annealing, (+) $T_{an} = 500\,^{\circ}C$ and (△) $T_{an} = 700\,^{\circ}C$.

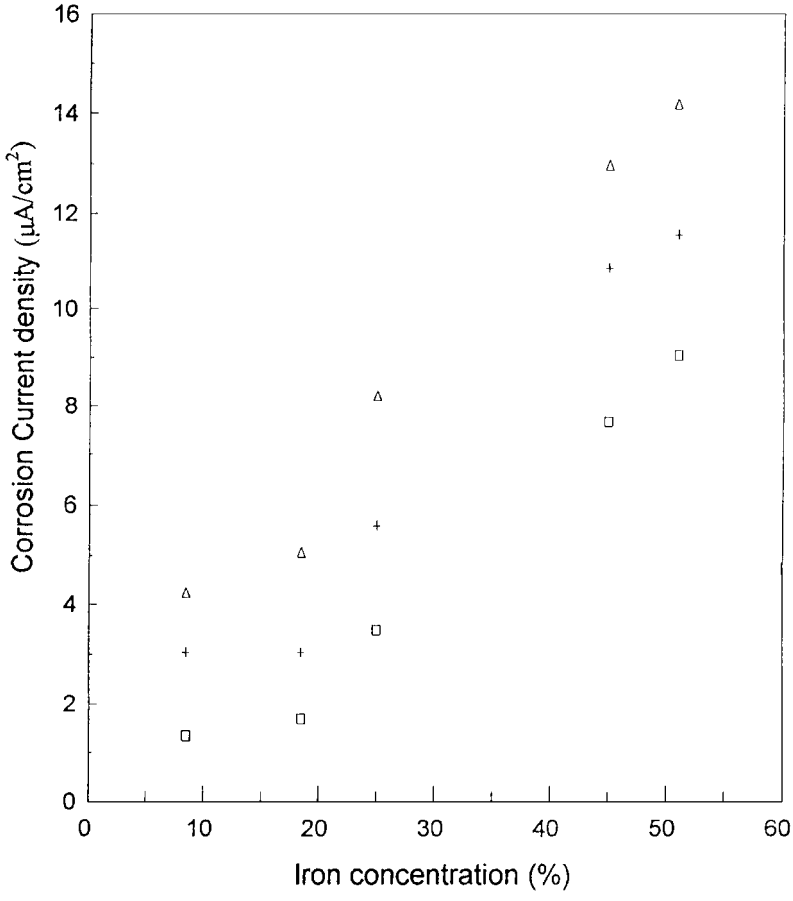

Figure 10 Corrosion current density vs. iron percentage of $Ni_{100-x}Fe_x$ alloys at $8.5 \leq x \leq 51$ immersed in 0.1 M Na_2SO_4 solution. (□) without annealing, (+) $T_{an} = 500\,^{\circ}C$ and (△) $T_{an} = 700\,^{\circ}C$.

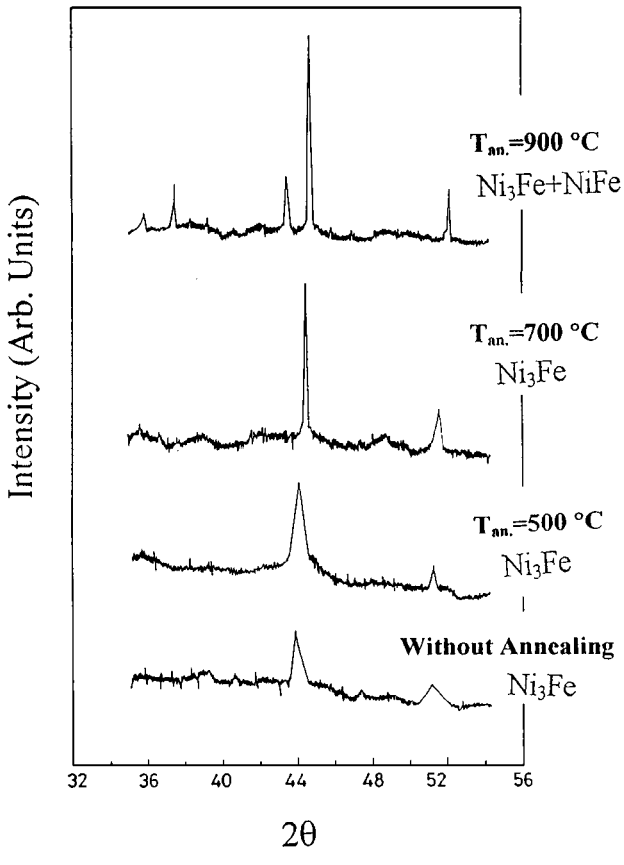

Figure 11 X-ray scan of $Ni_{74.5}Fe_{25.5}$ alloy with different annealing temperatures.

the iron content increases. This may be attributed to the fact that the increase of iron content factor plays a more dominant roles in determine the values of corrosion current.

3.2. Effects of annealing temperature (T_{an}) on the corrosion of $Ni_{100-x}Fe_x$ alloy

The relation between the concentration of iron and open-circuit potential for specimens with different annealing temperatures is shown in Fig. 2. The data show that $E_{o.c}$ shifts to lower values after annealing the samples, and also as the annealing temperature increases the corrosion tendency of the samples increases. From the polarization curves of all annealed samples, shown in Figs 5–9, the ratio between the corrosion current density after and before annealing $\{(i_{corr})_A/(i_{corr})_B\}$ and the ratio between the reciprocal value of the polarization resistance after and before annealing $\{(1/R_p)_A/(1/R_p)_B\}$ were calculated and listed in Table III. Fig. 10 represent the relation between the corrosion current density and Iron concentration at different annealing temperatures. From the figures, it is clear that there is a general enhancement of corrosion rates as a function of annealing temperature. These result indicate that the annealed samples at higher temperature obviously dissolve more rapidly compared to samples annealed at low temperature. The enhancement of the corrosion process for the annealed samples in Na_2SO_4 medium

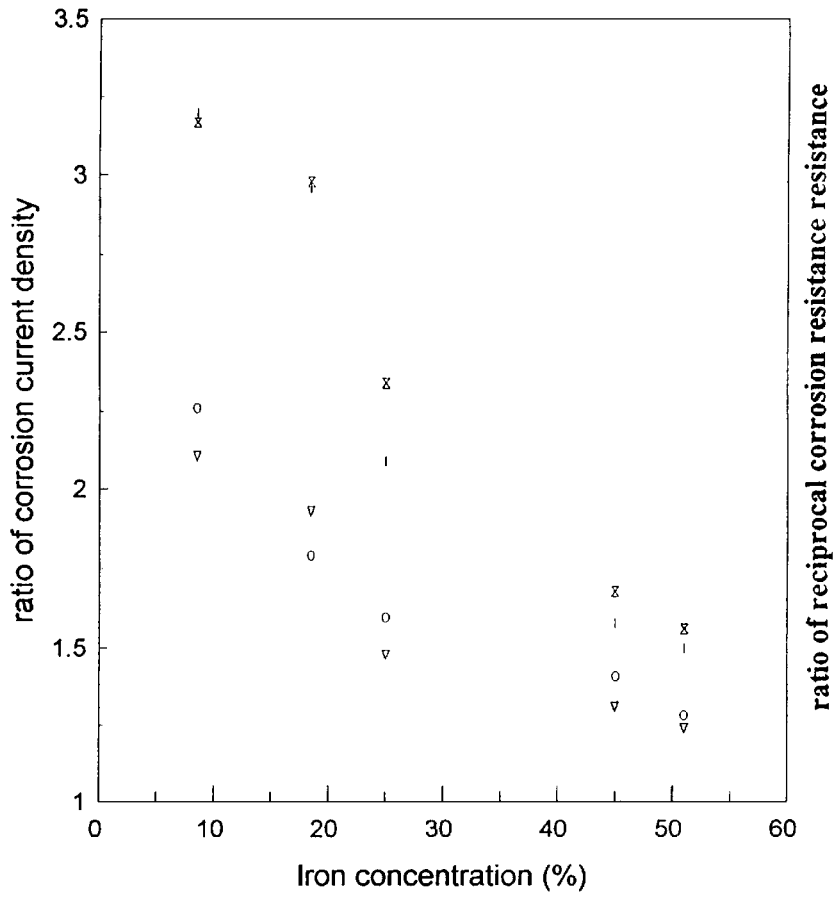

Figure 12 Corrosion current density ratio and reciprocal polarozation resistance ratio vs. iron concentration of $Ni_{100-x}Fe_x$ alloy. (○) $T_{an} = 500\,^{\circ}C$ and (⧖) $T_{an} = 700\,^{\circ}C$ (scale on left), (▽) $T_{an} = 500\,^{\circ}C$ and (|) $T_{an} = 700\,^{\circ}C$ (scale on right).

can be interpreted by the same manner in the X-ray data [16] (some X-ray diffractions are presented in Fig. 11 just to show the change in crystallinity). It the formation of crystallites in the sample due to the annealing process create grain boundaries through which dissolution of the material starts to take place. For better comparison between temperature of the annealing process and the reproducibility of the results obtaining by using potentiodynamic and linear polarization measurements, the corrosion current density ratio and the reciprocal polarization resistance ratio have been plotted against the iron concentration in Fig. 12. This figure indicates that the corrosion current density data obtained from the potentiodynamic technique are in a good agreement with reciprocal polarization resistance which obtained from the polarization resistance technique.

4. Conclusion

The corrosion results from the samples in Na_2SO_4 medium before annealing show that, the increase of the iron concentration leads to an increase in the corrosion rate. This result is unexpected since the increase of iron content increases the amorphousity of the sample and hence decreases the corrosion rate. But in this case there are two factors which affect the corrosion rate of the sample. The first one, tends to increase the corrosion rate due to the increase of iron content in the sample. While the second factor tends to decrease the corrosion rate due to the increase in the amorphous phase. The first factor plays a more dominant role in the corrosion mechanism. Moreover, as the annealing temperature increases the sample dissolves more rapidly. This enhancement of the corrosion rate id due to the formation of the crystallites by the annealing and the existence of the grain boundaries at which the dissolution of alloy starts to take place.

References

1. K. SUMIYAMA and Y. NAKAMURA, in "Rapidly Quenched Metals," edited by S. Sleeb and H. Warlimont (North-Holland, Amsterdam, 1985) p. 859.
2. S. MADER, *J. Vac. Sci. Technol.* **2** (1965) 35.
3. S. N. SRIMATHI, S. M. MAYANNA and B.S. SHESHADRI, *Surf. Technol.* **16** (1982) 277.
4. K. NAKAMURA, M. UMETANI and T. HAYASHI, *ibid.* **25** (1985) 111.
5. A. BRENNER, "Electrdeposianition of Alloys," Vol. 1 (Academic Press, New York, 1963) p. 77.
6. M. PERAKH, *J. Electrochem. Soc.* **122** (1975) 1260.
7. R. A. TREMMEL, *Plat. Surf. Finish.* **68**(2) (1981) 30.
8. V. HOLPUCH and J. VITEK, *Metalloberfläche* **36** (1982) 117.
9. K. NAKMURA and T. HAYASHI, *Bull. Univ. Osaka Prefect, Ser A* **32**(2) (1983) 127.
10. L. L. SHREIR (ed.), "Corrsion," Vol. 1 (Newnes-Butterworth, London, England, 1976) p. 1.
11. A. G. REVERZ and J. KRUGER, in "Passivity of Metals," edited by R. P. Frankenthal (Electrochem. Soc., Penington, NJ, 1978) p. 137.
12. N. NAKAMURA and T. HAYASHI, *Plat. Surf. Finish.* **72** (1985) 42.
13. E. KHAMIS, F. BELLUCCI, R. LATANISION and E. EL-ASHRY, *Corrosion* **47** (1991) 677.
14. F. MANSFELD and M. KENDING, *ibid.* **9** (1981) 545.
15. N. G. GOMAA, E. KHAMIS, A. AHAMED and S. ABAZA, *Werkstoffe und Korrosion* **45** (1994) 242.
16. To be published in J. Physics: condensed matter.

Received 2 April 1997
and accepted 14 September 1998